Technical Report

Removal Technology of Inclusion from Titanium Alloy Melt in Hearth

Hideo MIZUKAMI*
Tomoyuki KITAURA
Masaaki WADA
Shigeru UMEDA
Hitoshi FUNAGANE
Yoshinari TAKEDA
Yoshihisa SHIRAI

Abstract

Controlling the inclusion is necessary to improve the quality of titanium products. There are two types of inclusions in titanium: high-density inclusion (HDI) and low-density inclusion (LDI). Although HDI can be removed by settling out in a cold hearth, suspended LDI might flow out into the mold. The titanium nitride sponge that is a major source of LDI formed as a porous structure. From the predicted result for apparent density of the titanium nitride sponge, it was found that the sponge floats on titanium melt when the melt filled the pores of the sponge. To control flow behavior of LDI on the melt in a cold hearth, Marangoni flow was generated by electron beam irradiation near the pouring gate. The effect of electron beam irradiation was confirmed by both numerical simulation and experiment.

1. Introduction

Titanium has a strong affinity for oxygen. It is difficult to directly reduce the raw material or titanium ore. Titanium is hence usually produced by the Kroll process. The titanium ore is chlorinated, refined in the form of titanium tetrachloride ($TiCl_4$) to improve its purity, and then reduced with Mg to obtain a sponge-like titanium metal (titanium sponge).[1,2]

The titanium sponge is high-purity titanium (Ti ≥ 99.3%) and multiporous. To produce titanium, the titanium sponge is uniformly mixed with the necessary auxiliary materials (TiO_2, Fe, Al, etc.), heated to above titanium's melting point of 1941 K, melted, and cast into ingots. Inclusions (foreign matter) that inevitably enter the melted titanium sponge and auxiliary raw materials (hereinafter referred to as the raw melting materials) may remain in the ingots and cause quality defects in titanium products. These inclusions comprise low density inclusions (LDI) and high density inclusions (HDI). The LDI are mainly titanium nitrides. The titanium nitrides are formed from the partial nitrification of the titanium sponge mass obtained after $TiCl_4$ reduction and high-temperature vacuum separation or from the nitration of vapor deposited titanium produced by electron beam remelting described later. The HDI are broken pieces of tools used primarily to machine titanium ingots. These tools are made of Mo and W compounds. The density of these compounds is higher than that of molten titanium. Since these LDI and HDI have a higher melting point than titanium, they are not easily dissolved even in the molten titanium. The LDI and HDI are strictly controlled in the manufacturing steps until the titanium is melted. Given the possibility of the LDI and HDI flowing out into the mold, it is desirable that they can also be removed or rendered harmless in the melting step.

Titanium has a strong affinity for oxygen and has a high melting point. This means that the molten titanium cannot be contained by refractories (Al_2O_3, etc.) used in the refining and casting of carbon steel. For this reason, special melting methods such as consumable electrode vacuum arc remelting (VAR) and electron beam remelting (EBR) are used to melt titanium.[3,4]

With the VAR, a briquette is formed by the pressure compaction of the melting raw materials and used as a consumable electrode. The consumable electrode is heated and melted by a DC arc under a vacuum. The molten titanium directly drops into a water-cooled copper mold, forms a molten titanium pool, and sequentially solidifies into an ingot.

The EBR is a method of melting the raw melting materials by irradiating electron beams onto them. Since it became possible to manufacture large electron guns, the EBR is now being applied to the melting of mass production titanium for the following advantag-

* Senior Researcher, Dr.Eng., Titanium & Stainless-steel Research Dept., Materials Reliability Research Lab., Steel Research Laboratories
2-12-1 Minato-cho, Joetsu City, Niigata Pref. 942-8510

es over VAR:

(1) Scrap of various shapes can be used as a raw material.
(2) The mold has a degree of freedom regarding the cross-section shape and can directly cast rectangular parallelepiped slabs (hot rolling materials).
(3) The use of a cold hearth can settle out the HDI. The cold hearth is a water-cooled copper container filled with a titanium alloy of the same composition as the that of the titanium alloy to be melted and is designed to hold the molten titanium while the molten titanium is irradiated with electron beams.

In 2012, Nippon Steel Corporation introduced an EBR furnace at the Naoetsu Works (now the Naoetsu Area of the East Nippon Works) for the above reasons. Regarding the HDI removal capacity, a melting test was conducted by mixing 0.25 to 9.5 mm WC and Mo particles with the raw melting materials. X-ray radiography confirmed that all the HDI remained in the solidified cold hearth after the completion of melting.

Unlike the HDI, on the other hand, the LDI are not easily settled and removed in the molten titanium. This makes it difficult to evaluate their removal capacity. We must develop a melting and casting technology that can suppress the inflow of the LDI into the mold even if the LDI are mixed in the melting raw material and enter the cold hearth in the melting step.

Shiraki[5] installed two large cold hearths in a large EBR furnace to ensure the retention time for the dissolution and removal of the LDI. He also locally heated the molten titanium to produce a high temperature region. However, these measures require large cold hearths, many electron guns, and large vacuum chambers, increasing the equipment cost. In addition, he did not study the floating, flowing, and melting behaviors of the LDI in the molten titanium and did not evaluate the LDI removal capacity.

In this study, we investigated the floating and flowing behavior of the titanium nitride sponge as the LDI in the molten titanium in the EBR furnace, researched its morphology, and estimated its density. As a method of preventing the LDI from flowing out into the mold, we then evaluated by numerical analysis the effect of the Marangoni convection caused by intensively irradiating electron beams onto the surface of the molten titanium in the cold hearth. Furthermore, we tested the method of adding carbon rods as simulated LDI to the molten Ti-6Al-4V alloy in the EBR furnace and verified the effectiveness of the method in removing the LDI.

2. Electron Beam Remelting and Casting System

Figure 1 schematically illustrates the electron beam remelting and casting system installed in the Naoetsu Area of the East Japan Works. This system consists of an electron gun, a melting raw material feeder, a cold hearth, a mold, and an ingot withdrawal unit. These devices are placed in a vacuum vessel and operated in a vacuum atmosphere.

The raw melting materials are arranged in a container and pushed from behind and toward the cold hearth at a predetermined speed. When the end of the arranged raw materials reaches the wall surface position of the cold hearth, an electron beam is irradiated from above the end of the raw melting materials to melt them. Titanium is melted from the end of the raw melting materials pushed out at a constant speed, dropped into the cold hearth, and supplied through the pouring gate of the cold hearth into the mold. As the molten titanium solidifies into an ingot in the mold, the ingot is intermittently drawn downward.

We consider that the LDI mingled in the raw melting materials are undissolved by the electron beam irradiated onto the end of the raw melting materials, drop undissolved into the cold hearth, and enter the mold. The LDI trapped in the ingot cause streak-like defects in titanium sheets and break titanium wire rods during drawing. To prevent these defects, the LDI introduced into the cold hearth must not be allowed to flow out into the mold.

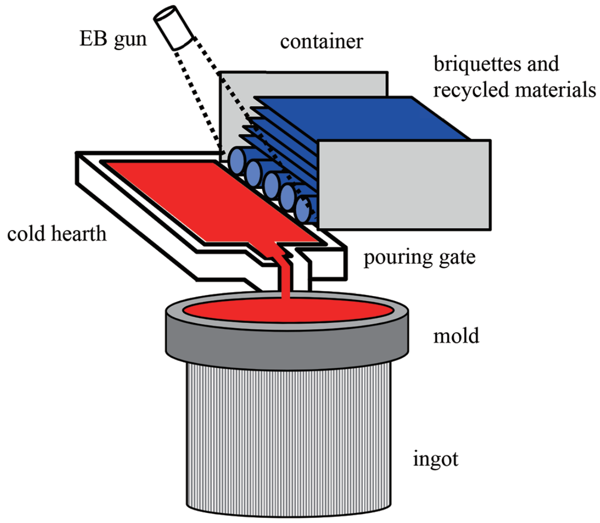

Fig. 1 Schematic diagram of melting and casting system in Naoetsu Area of East Nippon Works

3. Characteristics of Low Density Inclusions (LDI)

3.1 Structure of LDI

Typical examples of LDI are particles of nitrided sponge titanium or sponge titanium nitrided in the raw material production process. To understand the characteristics of the titanium nitride sponge, we nitrided sponge titanium and artificially produced the titanium nitride sponge. We observed the surface and cross-sectional microstructures of the nitrided sponge titanium samples.

Figure 2(a) shows a secondary electron beam image of the surface of a titanium nitride sponge sample. Figure 2(b) shows an optical micrograph of near the center of the cross section of the sample. From these observation results, we can see that the titanium nitride sponge has a porous structure and has a pore distance of about 50 μm.

To evaluate the porosity of the titanium nitride sponge, we measured it at room temperature by x-ray computed tomography. As a result, we found that the open porosity was 38% and the closed porosity was 0.1%. This means that the pores of the titanium nitride sponge were mostly open.

3.2 Apparent density of LDI

The porous titanium nitride sponge settles in the cold hearth if it is heavier than the molten titanium and floats and flows out into the mold if it is lighter than the molten titanium. To determine which condition applies, we must evaluate the apparent density of the titanium nitride sponge at the molten titanium temperature. However, it is difficult to directly measure the apparent density of the porous and idenfinite titanium nitride sponge.

In this study, we estimated the density of the titanium nitride sponge using dense titanium nitride and the following procedure. First, the true density (or density excluding pores) of dense titanium nitride at room temperature was estimated by the Archimedes meth-

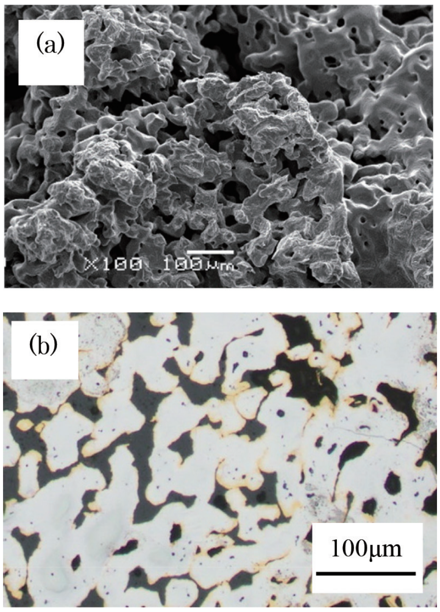

Fig. 2 (a) Surface and (b) center of cross section of titanium nitride sponge

od. Next, the density of the molten titanium at the liquidus temperature was calculated using the equation[6] for predicting the linear expansion coefficient of titanium nitride. Since the titanium nitride sponge has a porous structure, the calculated density was corrected for its porosity. The apparent density of the titanium nitride sponge was estimated accordingly.

Figure 3 shows the density of dense titanium nitride samples with different N concentrations at room temperature as measured by the Archimedes method. The density values reported in Reference 7) are also shown. We found that the density of titanium nitride increases as the N concentration increases. Next, the relationship between the density and the N concentration at a temperature of 1 977 K was calculated. This temperature corresponds to the liquidus temperature of the Ti-6Al-4V alloy. The density was converted by using the following relationship equation[6] among the linear expansion coefficient, temperature, and N concentration:

$$\alpha = \frac{\left(\left(1.2206+0.8348\times\frac{[N]}{[Ti]}\right)\times10^{-6}+\left(2.697-0.2256\times\frac{[N]}{[Ti]}\right)\times10^{-9}\times T\right)}{Lattice}$$

$$Lattice=0.41823+0.00530\times\frac{[N]}{[Ti]}+\left(1.2206+0.8348\times\frac{[N]}{[Ti]}\right)\times10^{-6}\times T$$
$$+\left(1.3485-0.1128\times\frac{[N]}{[Ti]}\right)\times10^{-9}\times T^2$$

where α is the linear expansion coefficient (K^{-1}) and T is the temperature (K).

Figure 4 shows the relationship between the apparent density and N concentration of the titanium nitride sponge at a temperature of 1 977 K and a porosity of 38%. The density of the titanium nitride sponge increases as the N concentration increases. Compared with the density of the molten Ti-6Al-4V alloy, the apparent density of the titanium nitride sponge is low when the molten titanium does not penetrate the pores of the titanium nitride sponge at all and is large when the molten titanium completely penetrates the pores of the titanium nitride sponge. This means that the titanium nitride sponge dropped into the cold hearth settles there if its pores are

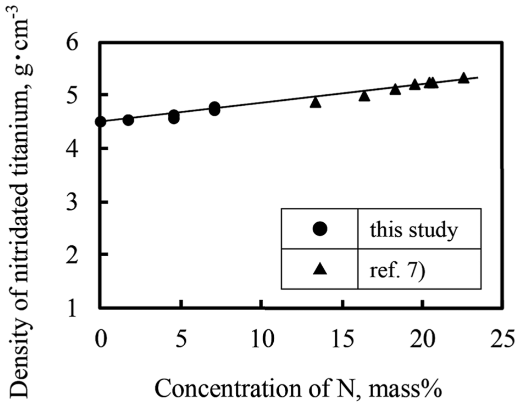

Fig. 3 Density of nitridated titanium at room temperature measured by Archimedes method

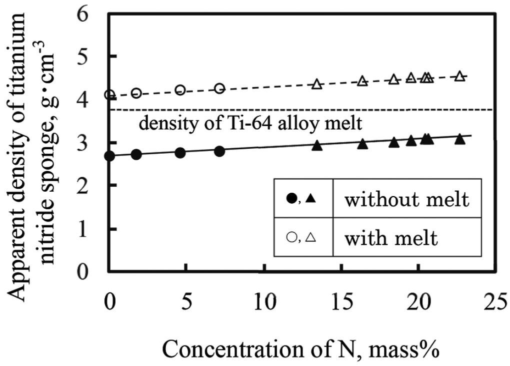

Fig. 4 Apparent density of titanium nitride sponge at liquidus temperature of Ti-6Al-4V alloy melt

filled with the molten titanium and floats to the molten titanium surface and flows out with the molten titanium if its pores are not filled with the molten titanium. To prevent the titanium nitride sponge from flowing into the mold, the floating titanium nitride sponge whose pores are not filled with the molten titanium should be prevented from moving in the cold hearth.

4. Calculation Method and Results

The behavior of the LDI floating on the molten titanium surface in the cold hearth was predicted by three-dimensional thermo-fluid analysis. This analysis set the strictest conditions for the LDI that the molten titanium does not penetrate the pores of the titanium nitride sponge and that the titanium nitride sponge is not dissolved (the particle size is always constant). We assumed that the flow of the molten titanium affects the behavior of the LDI but that the behavior of the LDI does not affect the flow of the molten titanium.

4.1 Numerical analysis model for alloy melt flow and LDI behavior

The flow velocity and temperature of the molten titanium were obtained by iteratively calculating the continuity equation (Equation (1)), the momentum equation (Equation (2)), the energy equation (Equation (4)), and the liquid fraction equation (Equation (6)). These equations were established under the following assumptions (a) to (c):

(a) The flow of the molten titanium is laminar.
(b) The natural convection caused by the change in density is

modeled by the Boussinesq approximation. This corresponds to the fourth term on the right side of Equation (2).

(c) The solidified region near the wall of the cold hearth is treated as a porous medium. The pressure loss caused by the presence of the solidified region is modeled by adding the momentum sink term to Equation (2). This corresponds to the fifth term on the right side of Equation (2). The volume fraction β of the liquid is zero in the completely solidified region, 1 in the liquid region, and between 0 and 1 in the other regions.

$$\nabla\cdot(\rho\vec{u})=0 \tag{1}$$

$$\nabla\cdot(\rho\vec{u}\vec{u})=-\nabla p+\nabla\cdot\bar{\bar{\tau}}+\rho\vec{g}-\rho\beta'(T-T_0)\vec{g}+\frac{(1-\beta)^2}{\beta^3+\varepsilon}A_{mesh}\vec{u} \tag{2}$$

$$\bar{\bar{\tau}}=\mu(\nabla\vec{u}+\nabla\vec{u}^T-\frac{2}{3}\nabla\cdot\vec{u}I) \tag{3}$$

$$\nabla\cdot(\rho\vec{u}H)=\nabla\cdot(\lambda\nabla T) \tag{4}$$

$$\mathrm{H}=c_pT+\beta L \tag{5}$$

$$\beta=\begin{cases}0 & \text{if } T<T_S\\ 1 & \text{if } T>T_L\\ \dfrac{T-T_S}{T_L-T_S} & \text{if } T_S<T<T_L\end{cases} \tag{6}$$

where ρ is the density, $\vec{u}$ is the flow velocity, p is the pressure, $\bar{\bar{\tau}}$ is the stress tensor calculated by Equation (3), $\vec{g}$ is the gravitational acceleration, β' is the thermal expansion coefficient, T is the temperature, T_0 is the reference temperature, β is the volume fraction of the liquid, ε is a very small value to avoid divergence (10^{-3}), A_{mesh} is a value of the mushy zone parameter as a constant (10^5), μ is the molecular viscosity, I is the unit matrix, H is the enthalpy expressed by Equation (5), λ is the thermal conductivity, c_p is the specific heat, L is the latent heat, T_S is the solidus temperature, and T_L is the liquidus temperature. The heat transfer coefficients between the molten titanium and the bottom and sides of the cold hearth were set to 1400 and 200 W/m^{2}K, respectively. **Table 1** shows the physical properties used in the analysis.

The LDI were regarded as particles. The behavior of the LDI was estimated by calculating the motion equation (Equation (7)) that considers the drag and buoyancy acting on the particles.

$$m_p\frac{d\vec{u}_p}{dt}=m_p\frac{\vec{u}-\vec{u}_p}{\tau_r}+m_p\frac{\vec{g}(\rho_p-\rho)}{\rho_p} \tag{7}$$

$$\tau_r=\frac{\rho_pd_p^2}{18\mu}\frac{24}{C_d\mathrm{Re}} \tag{8}$$

$$\mathrm{Re}\equiv\frac{\rho d_p|\vec{u}_p-\vec{u}|}{\mu} \tag{9}$$

$$C_D=C_1+\frac{C_2}{\mathrm{Re}}+\frac{C_3}{\mathrm{Re}^2} \tag{10}$$

where m_p is the particle mass, $\vec{u}_p$ is the particle velocity, ρ_p is the particle density (3440 kg/m^3), τ_r is the particle relaxation time expressed by Equation (8), d_p is the particle size (5.0 mm), Re is the relative Reynolds number defined by Equation (9), and C_D is the drag coefficient calculated by Equation (10). For the value of the coefficient C_i ($i=1-3$), we referred to the Reference 8). The surface tension gradient of the Marangoni stress was set to −0.00027 N/mK.

4.2 Analysis conditions

We considered the melting of the titanium nitride sponge in a rectangular water-cooled copper hearth (**Fig. 5**). We assumed two cases of electron beam irradiation. In one case, the electron beam was assumed not to be irradiated intensively on the entire molten titanium surface. (This pattern is hereinafter referred to as uniform irradiation.) In this case, the amount of heat input to the molten titanium surface by the electron beam irradiation was modeled by assigning the same heat flux value to all molten titanium surface positions. In the latter case, the entire molten titanium surface was assumed to be irradiated with the electron beam from an electron gun to prevent the solidification of the molten titanium. Another electron gun was assumed to be used to intensively irradiate the electron beam only at specific positions on the molten titanium surface. In this case, by referring to Reference 9), the heat flux on the molten titanium surface was modeled by such a Gaussian distribution (Equation (11)) that it would take the maximum value at the electron beam irradiation spot and would decay at other spots.

Table 1 Physical properties of melt

ρ	Apparent density (kg/m^3)	3820
c_P	Specific heat (J/kgK)	840
λ	Thermal conductivity (W/mK)	6.5 at 303 K 34.0 at 1973 K
μ	Molecular viscosity (kg/ms)	$0.03856-2.85243\cdot10^{-5}T$ $+5.45115\cdot10^{-9}T^2$
β'	Thermal expansion coefficient (1/K)	0.00018324
L	Latent heat (J/kg)	286000
T_S	Solidus temperature (K)	1967
T_L	Liquidus temperature (K)	1977

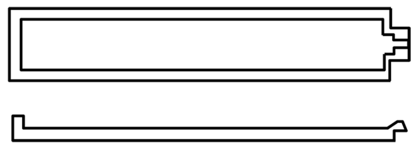

Fig. 5 Shape of cold hearth using analytical model

$$q_w=\alpha q_0\exp\left(-\frac{(x-x_0)^2+(y-y_0)^2}{2\sigma^2}\right) \tag{11}$$

$$Q=q_0\iint_{\substack{\text{all }x\\ \text{all }y}}\exp\left(-\frac{(x-x_0)^2+(y-y_0)^2}{2\sigma^2}\right)dxdy \tag{12}$$

where q_w is the heat flux on the molten titanium surface, α is the heat transfer efficiency (0.25), q_0 is the heat flux at the irradiation spot calculated by Equation (12), Q is the electron beam heat input (0.25 MW), (x, y) is the position on the molten titanium surface, (x_0, y_0) is the irradiation spot of the electron beam, and σ is the standard deviation (0.02 m).

The analysis used the commercial software ANSYS FLUENT. The PISO scheme was used for velocity-pressure coupling. The PRESTO! scheme was used for the pressure interpolation. A first order upwind scheme was used for the momentum interpolation. A second order upwind scheme was used for the temperature interpolation. The analysis assumed that the LDI were not dissolved (LDI particle size was always constant).

4.3 Analysis results

The analysis results of the molten titanium surface temperature, molten titanium surface flow, and LDI behavior are shown in **Fig. 6** and **Fig. 7**. The molten titanium is supplied to the left end of the cold hearth and discharged through the pouring gate on the right side. The number of LDI particles put into the molten titanium was 53. In the case of uniform irradiation, the flow on the molten titanium surface is from left to right (Fig. 6(b)). The LDI floating on the molten titanium surface move from left to right on this flow and reach the pouring gate without being blocked on the way (Fig. 6(c)).

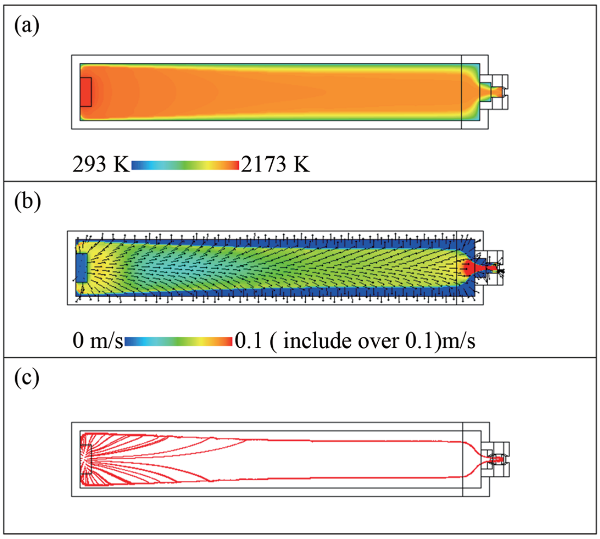

Fig. 6 Calculated results of surface temperature of melt, melt flow of surface, and behavior of LDI when electron beam was irradiated uniformly
(a) temperature of molten alloy surface, (b) surface flow velocity of molten alloy, and (c) behavior of LDI.

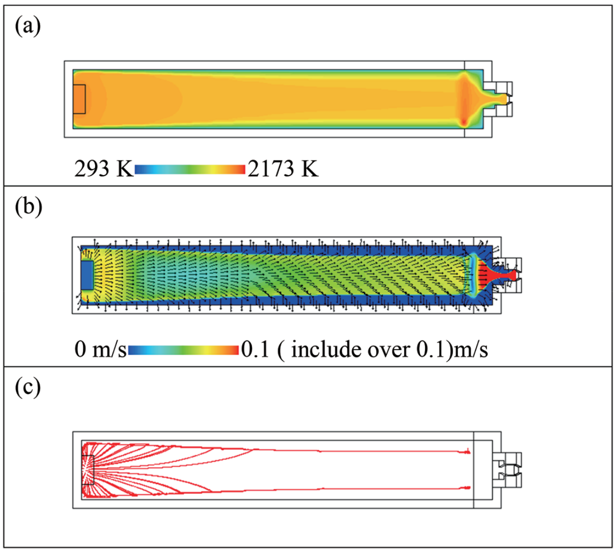

Fig. 7 Calculated results of surface temperature of melt, melt flow of surface, and behavior of LDI when electron beam was irradiated intensively
(a) temperature of molten alloy surface, (b) surface flow velocity of molten alloy, and (c) behavior of LDI.

When the electron beam is irradiated intensively, the molten titanium is heated in a region just before the pouring gate on the right side of the hearth (Fig. 7(a)). This region corresponds to the region where the electron beam is irradiated intensively. Since the Marangoni convection is induced by the temperature gradient with the surrounding region, a flow is formed toward the upstream side from the region where the electron beam is irradiated intensively (Fig. 7(b)). The Marangoni convection is a convection driven by the surface tension gradient resulting from the temperature difference. Due to this upward flow, the LDI that accompany the molten titanium flow from the upstream side are blocked in front of the intensive electron beam irradiation region as shown in Fig. 7(c).

The dissolution of the LDI is not considered in this analysis. Three of the present authors studied the dissolution rate of the titanium nitride sponge in detail.[10] Since the melting rate of the titanium nitride sponge is about 0.1 mm/s when the molten titanium temperature, one of the present analysis conditions, is 2136 K, it is estimated that the 5 mm in diameter titanium nitride sponge is dissolved in the molten titanium in several tens of seconds. For this reason, it is considered that while the LDI are blocked by the intensive electron beam irradiation, they are dissolved and removed or that the LDI are blocked in the semi-dissolved regions formed on the hearth sidewalls, captured, and removed.

5. Electron Beam Remelting (EBR) Test and Results

5.1 Experimental procedures

The numerical analysis predicted that the intensive irradiation of the electron beam on the molten titanium surface near the pouring gate of the cold hearth is effective in preventing the LDI floating on the molten titanium surface from flowing out into the mold.

To ascertain the effectiveness of the intensive electron beam irradiation in preventing the LDI from floating out into the mold, we ran an experiment by adding simulated inclusions.

As simulated inclusions, we selected $\varphi 10 \times 30$ mm carbon rods that are lower in density than the molten titanium, higher in melting point (sublimation point) than the temperature of the molten titanium, and difficult to react with the molten titanium.

The experiment used briquettes adjusted to the composition of the Ti-6Al-4V alloy as the raw melting materials. These briquettes were arranged in the raw material feeder and the carbon rods were placed in the gaps between the briquettes. When the electron beam is irradiated and the briquettes melt, the carbon rods fall into the cold hearth. The Marangoni convection was generated by providing an intensive electron beam irradiation region on the molten titanium surface near the pouring gate of the cold hearth.

5.2 Experimental results

Figure 8 (a) shows the observation results of the molten titanium surface in the cold hearth when the electron beam was not irradiated intensively. Carbon rods flowing from the upstream side of the cold hearth reached the pouring gate and flowed out into the mold.

Figure 8 (b) shows the observation results of the molten titanium surface when the electron beam was irradiated intensively on the molten titanium surface near the pouring gate of the cold hearth. A carbon rod that flowed from the upstream side of the cold hearth toward the pouring gate changed its direction at the position where the electron beam was irradiated intensively and flowed toward the side of the cold hearth. After that, the carbon rod was captured by the skull (solidified titanium) formed on the wall of the cold hearth and was successfully prevented from flowing out into the mold.

In this way, we were able to actually confirm that the intensive electron beam irradiation near the pouring gate of the cold hearth successfully prevents the floating LDI from flowing out into the mold.

6. Conclusions

We investigated the floating and flowing behaviors of the titanium nitride sponge as low-density inclusions (LDI) in the molten titanium in electron beam remelting (EBR) and investigated a method for preventing the titanium nitride sponge from flowing out into the mold. First, we evaluated by numerical analysis the effect of the Marangoni convection generated by the intensive electron beam ir-

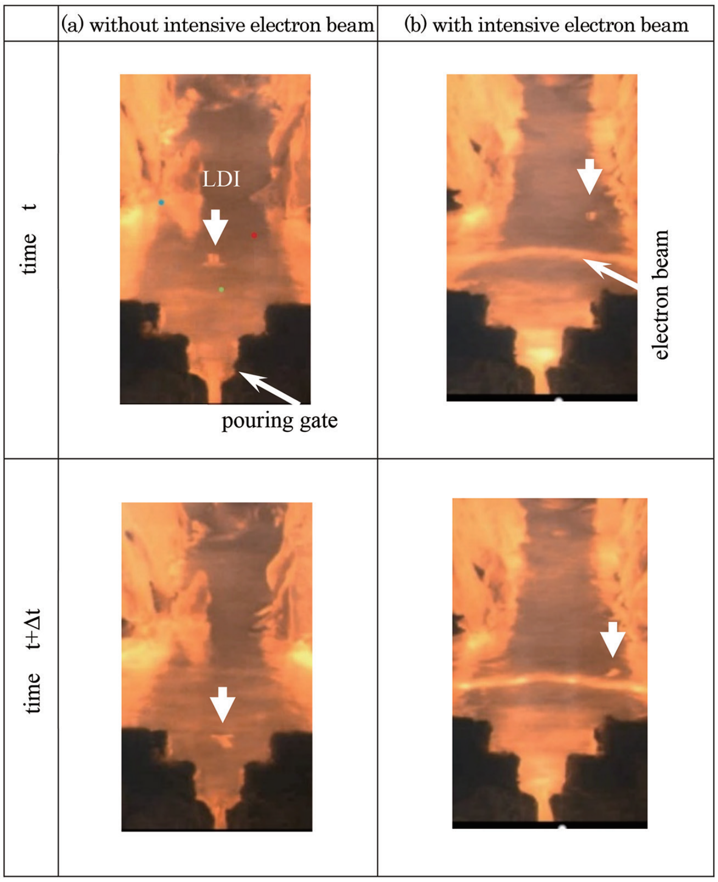

Fig. 8 Flow pattern of synthetic LDI in cold hearth with and without intensive electron beam

radiation on the molten titanium surface in the cold hearth. Also, we conducted the test of adding carbon rods as simulated LDI to the molten Ti-6Al-4V alloy in the EBR and verified the LDI removal effect.

(1) Titanium nitride sponge as the LDI has a porous structure of open pores. Its porosity was about 38%.

(2) The apparent density of titanium nitride sponge at the liquidus temperature of the Ti-6Al-4V alloy increased as the N concentration increased.

(3) When the molten titanium penetrated the pores of the titanium nitride sponge, the apparent density of the titanium nitride sponge was higher than the density of the molten titanium. When the molten titanium did not penetrate the pores of the titanium nitride sponge at all, the apparent density of the titanium nitride sponge was lower than the density of the molten titanium. These results showed that the titanium nitride sponge floats on the molten titanium surface.

(4) The numerical analysis revealed that the intensive irradiation of the electron beam near the pouring gate of the cold hearth successfully prevented the floating LDI from flowing out into the mold. Also, we conducted the EBR test of adding carbon rods as simulated LDI and confirmed the effect of intensive electron beam irradiation in preventing the carbon rods from flowing out into the mold.

References

1) Japan Titanium Society: Titanium Processing Technology. 1st Ed., Tokyo, Nikkan Kogyo Shimbun, 1992, p.2
2) Takeda, O., Okabe, T.: Journal of Japan Institute of Light Metals. 67, 257 (2017)
3) Niinomi, M., Nakai, M.: Journal of Japan Institute of Light Metals. 67, 307 (2017)
4) Japan Titanium Society: Series of Metallic Materials for Practical Use on Shop Floor: Titanium. 1st Ed., Tokyo, Kogyo Chosakai Publishing, 2007, p.168
5) Shiraki, T.: Titanium Japan. 69, 96 (2021)
6) Aigner, K., Lengauer, W., Rafaja, D., Ettmater, P.: J. Alloys Compounds. 215, 121 (1994)
7) Lengauer, W.: J. Alloys Compounds. 186, 293 (1992)
8) Morsi, S.A., Alexander, A.J.: J. Fluid Mech. 55, 193 (1972)
9) Zhao, X.: Master Thesis, The University of British Columbia, 2006
10) Mizukami, H., Kitaura, T., Shirai, Y.: ISIJ Int. 59, 102 (2019)

Hideo MIZUKAMI
Senior Researcher, Dr.Eng.
Titanium & Stainless-steel Research Dept.
Materials Reliability Research Lab.
Steel Research Laboratories
2-12-1 Minato-cho, Joetsu City, Niigata Pref. 942-8510

Hitoshi FUNAGANE
Senior Researcher, Dr.Eng.
Computational Engineering Research Dept.
Mathematical Science & Technology Research Lab.
Advanced Technology Research Laboratories

Tomoyuki KITAURA
Senior Manager, Head of Section, Dr.Eng.
Shape Products Making and Press Forging Technical Section, Titanium Production Technical Dept.
Titanium Production Div.
East Nippon Works Naoetsu Area

Yoshinari TAKEDA
Titanium Production Technical Dept.
Titanium Production Div.
East Nippon Works Naoetsu Area
(Current Manager, Head of Section,
Nippon Steel Naoetsu Titanium Corporation)

Masaaki WADA
Titanium Production Technical Dept.
Titanium Production Div.
East Nippon Works Naoetsu Area
(Current Manager, IP Strategy Dept.,
Intellectual Property Div.)

Yoshihisa SHIRAI
Senior Researcher
Titanium & Stainless-steel Research Dept.
Materials Reliability Research Lab.
Steel Research Laboratories
(Current Specialized Senior Manager, Technology & Sales Div., Amagasaki Unit, Nippon Steel Technology Co., Ltd.)

Shigeru UMEDA
Chief Manager
Titanium Technology Dept.
Titanium Technology Div.
Titanium Unit